bonding may contribute to the slower than expected rates of migration for phosphites.

Registry No. 1a, 119145-53-8; **1b**, 119145-55-0; **1c**, 119145-57-2; **1d**, 119145-59-4; **1e**, 119693-92-4; **1f**, 119145-61-8; **2a**, 109284-18-6; **2b**, 119145-65-2; **2c**, 119145-67-4; **2d**, 119145-69-6; **2e**, 119720-75-1; **2f**, 119145-71-0; **3**, 119645-38-1; [PPN][$Fe_2Co(CO)_9(CCO)$], 88657-64-1; [PPN][$Fe_2Co(CO)_8(PMe_2Ph)(CPMe_2Ph)$], 119694-40-5; [PPN]-[$Fe_2Co(CO)_8(P(OMe)_3)(CP(OMe)_3)$], 119694-42-7; Co, 7440-48-4; Fe, 7439-89-6.

Novel Hydrolysis Pathways of Dimesityldifluorosilane via an Anionic Five-Coordinated Silicate and a Hydrogen-Bonded Bisilonate. Model Intermediates in the Sol-Gel Process[1,2]

Stephen E. Johnson,[3] Joan A. Deiters,[4] Roberta O. Day, and Robert R. Holmes*

Contribution from the Department of Chemistry, University of Massachusetts, Amherst, Massachusetts 01003. *Received July 29, 1988*

Abstract: Reaction of dimesityldifluorosilane, Mes_2SiF_2, with $Et_4NF\cdot 2H_2O$ in acetonitrile resulted in the formation of the five-coordinated complexes, [Et_4N][Mes_2SiF_3], [Et_4N][$MesSiF_4$], the hydrogen bisilonate, [$Mes_2Si(F)O]_2$[H][Et_4N] (**2**), and the disiloxane, $(Mes_2SiF)_2O$ (**3**). Each of these products was isolated as a crystalline compound and characterized by solution state ^1H, ^{19}F, and ^{29}Si NMR spectroscopy. The X-ray structure of [Mes_2SiF_3][K,18-crown-6]$\cdot CH_2Cl_2$ (**1**) as well as that of **2** and **3** were determined. The hydrolysis pathway of Mes_2SiF_2 involves the intermediates, $Mes_2SiF_3^-$ and $Mes_2Si(F)$-O-H-OSi(F)Mes_2^-, on the way to the disiloxane **3**. This pathway is used as a model for the initial hydrolysis of silicic acid in the sol-gel process. Ab initio calculations are presented showing that this process which results in the formation of the disiloxane, $(HO)_3Si$-O-$Si(OH)_3$, is one of low energy. The importance of anionic pentacoordinate silicon and the hydrogen-bonded bisilonate in the hydrolytic sequence is stressed. The silicate **1** crystallizes in the monoclinic space group $P2/c$ with a = 16.636 (5) Å, b = 15.035 (3) Å, c = 15.720 (4) Å, β = 110.98 (2)°, and Z = 4. The hydrogen bisilonate **2** crystallizes in the monoclinic space group $P2_1/n$ with a = 8.567 (2) Å, b = 9.479 (3) Å, c = 26.754 (5) Å, β = 96.06 (2)°, and Z = 2. The disiloxane **3** crystallizes in the monoclinic space group $C2/c$ with a = 14.337 (2) Å, b = 12.458 (4) Å, c = 18.577 (4) Å, β = 92.31 (1)°, and Z = 4. The final conventional unweighted residuals are 0.088 (**1**), 0.065 (**2**), and 0.048 (**3**).

Previous work[5-9] has demonstrated the formation of five-coordinated anionic fluorosilicates, $R_nSiF_{5-n}^-$ (n = 0, 1, 2, 3), isoelectronic with phosphoranes. These acyclic derivatives result largely from the reaction of fluoride ion with the four-coordinated fluorosilane precursor. For example, [Ph_2(**1**-Np)SiF_2][$S(NMe_2)_3$][9] is formed by treating Ph_2(**1**-Np)$SiNMe_2$ with SF_4 in ether solution, and [t-$BuPhSiF_3$][$C_{12}H_{24}O_6K$][10] results from the reaction of t-$BuPhSiF_2$ with KF, and 18-crown-6 in acetonitrile. Like phosphoranes,[11,12] the molecular structures of all acyclic derivatives[6,7,9,10] studied so far exhibit only modest distortions from the basic trigonal bipyramidal geometry. This is in contrast to corresponding cyclic derivatives of pentacoordinated silicon[13-18] and phosphorus[11,18-19] which show a range of X-ray structures extending from the trigonal bipyramid to the square or rectangular pyramid along the Berry pseudorotational coordinate.[20]

Recently, some studies have been directed toward the reaction chemistry of the five-coordinated acyclic silicates. For example, Corriu and co-workers[21a] found that in alkylation reactions of diorganodifluorosilanes Grignard reactions were more facile when conducted with the five-coordinated anions $R_2SiF_3^-$ compared to direct reactions with the corresponding R_2SiF_2 derivatives.

$$[R_2SiF_3][K,18\text{-crown-}6] + R'MgX \rightarrow R_2R'SiF + MgXF + [K,18\text{-crown-}6]F \quad (1)$$

Recent work by Sakurai and co-workers[21b,c] also support the unique reactivity of five-coordinated anionic silicates in the allylation of aldehydes.

In somewhat analogous fashion, we find that dimesityldifluorosilane does not react with water in refluxing acetonitrile. However, rapid reaction occurs when the tetraethylammonium fluoride hydrate is introduced. Presumably, $Mes_2SiF_3^-$ forms which then acts as the reactive species. In the process, a number of products are indicated. The investigation of this hydrolysis reaction forms the principal topic of the present paper. In the course of the study, the X-ray structures of three of the resultant products were determined. These are [Mes_2SiF_3][K,18-c-6]$\cdot$ CH_2Cl_2 (**1**), [$Mes_2Si(F)O]_2$[H][Et_4N] (**2**), and $(Mes_2SiF)_2O$ (**3**).

(1) Pentacoordinated Molecules. 76. Part 75: Holmes, R. R.; Day, R. O.; Payne, J. S. *Phosphorus, Sulfur, and Silicon* **1989**, *42*, 1. In this paper, the term silonate is used to represent the monoanion of silanetriol.
(2) Presented in part at the 194th National Meeting of the American Chemical Society, New Orleans, LA, August 1987; paper INOR 20.
(3) This work represents in part a portion of: Johnson, S. E., Ph.D. Thesis, University of Massachusetts, Amherst, MA, 1989.
(4) Department of Chemistry, Vassar College, Poughkeepsie, NY 12601.
(5) Klanberg, F.; Muetterties, E. L. *Inorg. Chem.* **1968**, *7*, 155.
(6) Schomburg, D.; Krebs, R. *Inorg. Chem.* **1984**, *23*, 1378.
(7) Schomburg, D. *J. Organomet. Chem.* **1981**, *221*, 137.
(8) Damrauer, R.; Danahey, S. E. *Organometallics* **1986**, *5*, 1490.
(9) Harland, J. J.; Payne, J. S.; Day, R. O.; Holmes, R. R. *Inorg. Chem.* **1987**, *26*, 760.
(10) Payne, J. S., Ph.D. Thesis, University of Massachusetts, Amherst, MA, 1989.
(11) Holmes, R. R. *Pentacoordinated Phosphorus—Structure and Spectroscopy*; ACS Monograph 175; American Chemical Society: Washington, DC, 1980; Chapter 2.
(12) Macho, C.; Minkwitz, R.; Rohmann, J.; Steger, B.; Wölfel, V.; Oberhammer, H. *Inorg. Chem.* **1986**, *25*, 2828.
(13) Harland, J. J.; Day, R. O.; Vollano, J. F.; Sau, A. C.; Holmes, R. R. *J. Am. Chem. Soc.* **1981**, *103*, 5269.
(14) Holmes, R. R.; Day, R. O.; Harland, J. J.; Sau, A. C.; Holmes, J. M. *Organometallics* **1984**, *3*, 341.
(15) Holmes, R. R.; Day, R. O.; Harland, J. J.; Holmes, J. M. *Organometallics* **1984**, *3*, 347.
(16) Holmes, R. R.; Day, R. O.; Chandrasekhar, V.; Holmes, J. M. *Inorg. Chem.* **1985**, *24*, 2009.
(17) Holmes, R. R.; Day, R. O.; Chandrasekhar, V.; Harland, J. J.; Holmes, J. M. *Inorg. Chem.* **1985**, *24*, 2016.
(18) Holmes, R. R. *Prog. Inorg. Chem.* **1984**, *32*, Chapter 2.
(19) (a) Holmes, R. R.; Deiters, J. A. *J. Am. Chem. Soc.* **1977**, *99*, 3318; (b) Holmes, R. R. *Acc. Chem. Res.* **1979**, *12*, 257 and references cited therein.
(20) Berry, R. S. *J. Chem. Phys.* **1960**, *32*, 933.
(21) (a) Corriu, R. J. P.; Guerin, C.; Henner, B. J. L.; Wong Chi Man, W. W. C. *Organometallics* **1988**, *7*, 237. (b) Kira, M.; Kobayashi, M.; Sakurai, H. *Tetrahedron Lett.* **1987**, *28*, 4081. (c) Kira, M.; Sato, K.; Sakurai, H. *J. Am. Chem. Soc.* **1988**, *110*, 4599. Likewise, facile reactions take place under mild conditions between cyclic containing anionic pentacoordinated silicon compounds and a variety of organic derivatives, e.g., aldehydes and ketones: Kira, M.; Sato, K.; Sakurai, H. *J. Org. Chem.* **1987**, *52*, 948; *Chem. Lett. Chem. Soc. Jpn.* **1987**, 2243. Hosomi, A.; Kohra, S.; Tominaga, Y. *J. Chem. Soc., Chem. Commun.* **1987**, 1517.

0002-7863/89/1511-3250$01.50/0

^{19}F and ^{29}Si NMR spectra established their solution state behavior.

As a consequence of this work, a plausible model for the initial stages of hydrolysis of silicic acid, $Si(OH)_4$, in the sol-gel process[22] is suggested leading to the formation of disiloxane units, $(HO)_3Si$-O-$Si(OH)_3$. To ascertain the feasibility of the model, ab initio calculations employing GAUSSIAN 86 basis sets were performed. The results of these calculations also are presented here.

Experimental Section

General Methods. Vacuum-line and Schlenk techniques were used for the preparation and purification of reactants and products.[23] All the reactions studied were performed under an argon atmosphere, unless otherwise noted. The Grignard reagents, mesityl magnesium bromide, and *o*-tolyl magnesium bromide (Aldrich) were stored under argon prior to use. Methylene chloride and toluene solvents were dried by reflux over CaH_2. Acetonitrile was dried by reflux over P_2O_5. ^{29}Si (59.59 MHz), ^{19}F (282.2 MHz), and ^1H (299.9 MHz) pulse Fourier transform NMR spectra were recorded on a Varian Associates Corp. XL-300 spectrometer. Data manipulation utilized standard Varian software with a VXR series data system. ^1H and ^{29}Si chemical shifts are reported relative to Me_4Si. ^{19}F chemical shifts are reported relative to $CFCl_3$. All are in ppm. Variable temperature experiments were carried out in methylene-d_2 chloride solvent (Aldrich). Temperature calibration was accomplished by using a standard ethylene glycol sample with a calibration error of ± 0.5 °C. ^{29}Si NMR experiments were performed with INEPT programs[24] as well as standard pulse programs. IR spectra were recorded on a PE 783 instrument.

Preparation of Dimesityldifluorosilane, Mes_2SiF_2. The preparation of this organofluorosilane is based on the modification of a procedure described by Neruda and Wiberg.[25a] Tetrafluorosilane (41.64 g, 400 mmol) was passed through 100 mL of a 1.0 M solution of 2-mesitylmagnesium bromide (19.91 g, 100 mmol) in THF for 2 h. The mixture was heated to reflux, maintaining the reflux 3 h after the addition of SiF_4 was complete. The mixture was allowed to cool, and the THF solution was concentrated. The crystalline precipitate that formed on standing was collected by vacuum filtration. Recrystallization from CH_2Cl_2 yielded colorless crystals. The filtrate was washed with water, and any remaining Mes_2SiF_2 was extracted with CH_2Cl_2. A total of 12.3 g (81% yield) of colorless, crystalline Mes_2SiF_2 was obtained, mp 145–147 °C: ^1H NMR ($CDCl_3$) 2.27 (s, 6 H, *p*-Me), 2.37 (s, 12 H, *o*-Me), 6.84 (s, 4 H, *m*-H; aromatic ring); ^{19}F NMR ($CDCl_3$) at 25 °C −123.5 (d, J_{SiF} = 297 Hz); ^{29}Si NMR ($CDCl_3$) at 25 °C −23.31 (t, J_{SiF} = 299 Hz). Anal. Calcd for $C_{18}H_{22}SiF_2$: C, 71.00; H, 7.30. Found: 70.99; H, 7.36.

Reaction of Dimesityldifluorosilane, Mes_2SiF_2, with Tetraethylammonium Fluoride Dihydrate. Tetraethylammonium fluoride dihydrate (1.12 g, 7.48 mmol) was dissolved in 10 mL of acetonitrile, followed by 3 mL of 2,2-dimethoxypropane (DMP). This solution was stirred for 1 h prior to addition. The latter solution was slowly added to a solution of Mes_2SiF_2 (2.28 g, 7.48 mmol) in 25 mL of acetonitrile resulting in an exothermic reaction. Precipitate formation was observed within 30 min of the addition. The precipitate was collected by vacuum filtration immediately after formation. A total of 0.94 g of white precipitate was collected, exhibiting a broad mp range 128–151 °C. The material dissolved in $CDCl_3$ and its ^{19}F NMR was checked: ^{19}F NMR ($CDCl_3$) −74.2, −124.1, $Mes_2SiF_3^-$; −110.6, J_{SiF} = 218 Hz, $MesSiF_4^-$; −120.9, J_{SiF} = 287 Hz, $(Mes_2SiF)_2O$; −123.5, Mes_2SiF_2; −130.1, J_{SiF} = 111 Hz, $[Mes_2Si(F)O]_2[H][Et_4N]$; −157.5. The assignments given here are based on the isolation and independent NMR characterization of each product that is described in the following preparations.

Preparation of Potassium 18-Crown-6 Dimesityltrifluorosilicate [K,18-c-6][Mes_2SiF_3] (1). Dimesityldifluorosilane (2.29 g, 7.52 mmol), 18-crown-6 (1.99 g, 7.52 mmol), and KF (0.437 g, 7.52 mmol) were reacted in 20 mL of toluene at room temperature with stirring. Precipitate formation was observed shortly after mixing the reactants. The reaction was allowed to stir for 24 h. The white precipitate that formed was collected by vacuum filtration and washed with toluene. The precipitate was recrystallized from CH_2Cl_2/benzene to yield 3.77 g (80% yield) of crystalline material, mp 175–178 °C (dec). The precipitate dissolves in CH_2Cl_2 alone to form a solvent adduct, mp 178–180 °C (dec). These crystals readily lose solvent when exposed to the atmosphere. The compound was characterized without solvent and as a methylene chloride adduct. **[K-18-crown-6][Mes_2SiF_3].** ^1H NMR ($CDCl_3$), 20 °C, 2.22 (s, 6 H, *p*-Me), 2.49 (s, 12 H, *o*-Me), 6.60–6.85 (m, 4 H, *m*-H; aromatic ring). Anal. Calcd for $C_{30}H_{46}SiF_3O_6K$: C, 57.47; H, 7.41. Found: C, 57.40; H, 7.53.

[K-18-crown-6][Mes_2SiF_3]·CH_2Cl_2 (1). ^1H NMR ($CDCl_3$), 20 °C, 2.22 (s, 6 H, *p*-Me), 2.49 (s, 12 H, *o*-Me), 3.52 (s, 24 H, -OCH_2CH_2O-), 5.30 (s, 2 H, CH_2Cl_2), 6.60–6.85 (m, 4 H, *m*-H; aromatic ring); ^{19}F NMR (CD_2Cl_2), 20 °C, −77.80 (br s, $2F_a$), −126.7 (br s, F_e); ^{19}F NMR (CD_2Cl_2), −70 °C, −79.23 (d, $2F_a$, J_{SiF} = 259 Hz), −127.7 (t, F_e, J_{SiF} = 219 Hz); ^{29}Si NMR (CD_2Cl_2), 20 °C, −92.5 (q, J_{SiF} = 247 Hz); ^{29}Si NMR (CD_2Cl_2), −70 °C, −92.5 (d of t, J_{SiF} = 262 Hz, J_{SiF} = 219 Hz).

Isolation of Tetraethylammonium Tetramesityl-1,3-difluorohydrogenbisilonate, $[Mes_2Si(F)O]_2[H][Et_4N]$ (2). A solution of tetraethylammonium fluoride dihydrate (1.12 g, 7.48 mmol) in 7 mL of acetonitrile and 3 mL of 2,2-dimethoxypropane was prepared. This solution was added to a solution of dimesityldifluorosilane (2.28 g, 7.48 mmol) in 25 mL of acetonitrile. The reactants were stirred for 24 h at room temperature. The solution was concentrated on a rotary evaporator and cooled. The first crop of crystals collected was $(Mes_2SiF)_2O$ (3) identified by its mp, 152–155 °C. The filtrate was concentrated further and cooled. A small amount of crystalline $[Mes_2SiF_3][Et_4N]$ was isolated (0.4 g), mp 190–194 °C (dec). These needles were very hygroscopic, decomposing when exposed to atmosphere within seconds: ^1H NMR ($CDCl_3$) 1.11 (t, methyl protons Et_4N, 12 H), 2.19 (s, *p*-Me, 6 H), 2.36 (s, *o*-Me, 12 H), 3.02 (q, methylene protons Et_4N, 8 H), 6.61–6.92 (m, *m*-H or aromatic ring, 4 H); ^{19}F ($CDCl_3$) −74.43 (br s, F_{ax}, 2 F), −124.1 (br s, F_{eq}, 1 F). Recrystallization of this compound from acetonitrile resulted in the isolation of **2**, as crystalline plates from acetonitrile, mp > 250 °C. The yield of **2**, based on Mes_2SiF_3, is 8%. The bisilonate anion is very hygroscopic. The crystalline plates convert to $(Mes_2SiF)_2O$ (3) upon exposure to atmospheric moisture or recrystallization from wet acetonitrile. Compound **2** was characterized as follows: ^1H NMR (CD_3CN), −20 °C, 1.31 (t, 12 H, CH_3-), 2.31 (s, 12 H, *p*-Me), 2.48 (s, 24 H, *o*-Me), 2.07 (m, 1 H, O—H—O, J_{HF} = 2.2 Hz), 3.12 (q, 8 H, -CH_2-), 6.79 (s, 8 H, *m*-H, aromatic ring); ^{19}F NMR (CD_3CN), 20 °C, −125.9 (d, J_{SiF} = 110 Hz); ^{29}Si NMR (CD_3CN), 20 °C, −33.84 (d, J_{SiF} = 115 Hz). Anal. Calcd for $C_{44}H_{65}Si_2F_2O_2N$: C, 71.97; H, 8.94. Found: C, 72.07; H, 8.65.

Preparation of Tetramesityl-1,3-difluorodisiloxane, $(Mes_2SiF)_2O$ (3). Dimesityldifluorosilane (1.99 g, 6.54 mmol) was reacted with a solution containing $Et_4NF·2H_2O$ (1.21 g, 6.54 mmol) in 50 mL of acetonitrile. Afterwards, the mixture was allowed to stir at room temperature for 24 h. The clear solution was concentrated on a rotary evaporator. Cooling the concentrate resulted in the formation of clear colorless crystals, mp 152–155 °C. A total of 1.34 g of **3** was collected (71% yield). The IR spectrum of a Nujol mull showed no band in the OH stretching region: ^1H NMR ($CDCl_3$), 20 °C, 2.22 (s, 12 H, *p*-Me), 2.50 (s, 24 H, *o*-Me), 6.69 (s, 8 H, *m*-H, aromatic ring); ^{19}F NMR ($CDCl_3$), 20 °C, −120.9 (d, J_{SiF} = 287 Hz); ^{29}Si NMR ($CDCl_3$), 20 °C, −31.53 (d, J_{SiF} = 287 Hz). Anal. Calcd for $C_{36}H_{44}Si_2F_2O$: C, 73.66; H, 7.57. Found: C, 73.40; H, 7.70.

Reaction of [Mes_2SiF_3][K,18-crown-6] with Water. A solution of [Mes_2SiF_3][K,18-crown-6] (1.54 g, 2.45 mmol) in 10 mL of CH_3CN was reacted with 0.1 mL of H_2O at 25 °C. Immediate formation of a white precipitate was observed. The mixture was stirred for 24 h at room temperature. The small amount of precipitate that formed was collected. The filtrate was concentrated on a rotary evaporator. Cooling the concentrate resulted in the formation of clear colorless crystals. Both the initial precipitate and the crystalline material from the filtrate were recrystallized from CH_2Cl_2 to give $(Mes_2SiF)_2O$ (3) (yield 0.92 g, 62%) characterized as described above by ^1H, ^{19}F, and ^{29}Si NMR.

Comparative Rate Study of Hydrolysis of [Mes_2SiF_3][K,18-crown-6] and Mes_2SiF_2 in Acetone. Solutions of [Mes_2SiF_3][K,18-crown-6] in acetone-d_6 and solutions of Mes_2SiF_2 in acetone-d_6 were prepared for hydrolysis with added water. The composition of the solutions is listed in Table I. This resulted in mixtures in which the molar concentrations of water reacting with silicon compound varied from 1:1 to 2:1 to 10:1. A typical procedure is outlined here for the first entry in Table I.

A 0.240 M solution of [Mes_2SiF_3][K,18-crown-6] (0.256 g, 0.408 mmol) in 1.7 mL of acetone-d_6 was prepared. An equivalent amount of H_2O (7.36 mL, 0.408 mmol) was added via a syringe. The solution was mixed vigorously, and its ^{19}F NMR spectra were recorded at intervals of 5.0 min for 2 h with a final spectrum recorded after 24 h.

Preparation of $Mes_2SiF(OH)$. Dimesityldifluorosilane (5.08 g, 16.7 mmol) was added to an equivalent amount of a 25% solution of Et_4NOH (9.82 g, 16.7 mmol) in methanol. The reactants were stirred, and then the mixture was heated to reflux. The reflux was maintained 1 h, after

(22) (a) Iler, R. K. *The Chemistry of Silica*; John Wiley and Sons: New York, 1979. (b) Shimono, T.; Isobe, T.; Tarutani, T. *J. Chromatogr.* **1983**, *258*, 73. (c) Okkerse, C. Porous Silica. In *Physical and Chemical Aspects of Adsorbents and Catalysts*; Linsen, B. G., Ed.; Academic Press: New York, 1970; Chapter 5.

(23) Shriver, D. F.; Drezdzon, M. A. *The Manipulation of Air-Sensitive Compounds*, 2nd ed.; John Wiley and Sons: New York, 1986.

(24) Blinka, T. A.; Helmer, B. J.; West, R. *Adv. Organomet. Chem.* **1984**, *23*, 193 and references cited therein.

(25) (a) Wiberg, N.; Neruda, B. *Chem. Ber.* **1966**, *99*, 740. (b) Eaborn, C. *J. Chem. Soc.* **1952**, 2840.

Table I. Solution Concentrations for Reaction of $[Mes_2SiF_3][K,18\text{-}c\text{-}6]$ and Mes_2SiF_2 with Water

$[Mes_2SiF_3]$-[K,18-c-6]		acetone-d_6,	$[Mes_2SiF_3]$-	H_2O added	
g	mmol	mL	[K,18-c-6], M	μL	mmol
0.256	0.408	1.7	0.240	7.36	0.408
0.270	0.431	1.8	0.239	15.5	0.859
0.266	0.424	1.8	0.236	76.5	4.24
Mes_2SiF_2				H_2O added	
g	mmol	acetone-d_6	Mes_2SiF_2	μL	mmol
0.124	0.407	1.1	0.370	7.34	0.407
0.190	0.624	1.7	0.367	22.5	1.25
0.157	0.516	1.4	0.368	92.9	5.16

which the mixture was allowed to cool. A white precipitate formed. The precipitate was collected by vacuum filtration. The white powder was recrystallized from methylene chloride to yield 3.10 g of colorless crystals of $Mes_2Si(OH)F$, mp 155–158 °C. The filtrate was concentrated, and an additional 0.72 g of the compound was isolated. A total of 3.82 g of $Mes_2Si(F)OH$ was isolated (76% yield). The IR spectrum of a Nujol mull showed the presence of ν(OH) at 3410 cm^{-1} as a broad band: ^{1}H ($CDCl_3$) 2.24 (s, p-Me, 6 H), 2.26 (s, o-Me, 12 H), 2.38 (s, OH, 1 H), 6.70–6.76 (m, aromatic ring protons, 4 H); ^{19}F ($CDCl_3$) −120.9 (d$_{Si}$, J_{SiF} = 287 Hz); ^{29}Si ($CDCl_3$) −31.47 (d$_F$, J_{SiF} = 287 Hz). Anal. Calcd for $C_{18}H_{23}SiFO$: C, 71.46; H, 7.68. Found: C, 71.01; H, 7.61.

Isolation of Tetraethylammonium Mesityltetrafluorosilicate $[Et_4N][MesSiF_4]$ (4). A solution of tetraethylammonium fluoride dihydrate (1.53 g, 8.28 mmol) in 20 mL of CH_3CN was prepared. This solution was added to a solution of dimesityldifluorosilane (2.52 g, 8.28 mmol) in 15 mL of CH_3CN. The reactants were mixed and heated to reflux. The reflux was maintained 3 h, and then the mixture was allowed to cool. A small amount of white precipitate was collected. The filtrate was concentrated on the rotary evaporator. Colorless crystalline material had formed from the concentrated solution having a mp > 250 °C. The total yield of $[Et_4N][MesSiF_4]$ (4) isolated was 2.20 g (46% yield). The compound was characterized as follows: ^{1}H NMR (acetone-d_6) at 20 °C 1.31 (t, 12 H, CH_3-), 2.17 (s, 3 H, p-Me), 2.48 (s, 6 H, o-Me), 3.11 (q, 8 H, -CH_2-), 6.64 (s, 2 H, m-H, aromatic ring); ^{19}F NMR (acetone-d_6) at 20 °C −111.1 (d, J_{SiF} = 216 Hz); ^{29}Si NMR (acetone-d_6) at 20 °C −120.6 (p, J_{SiF} = 216 Hz). Anal. Calcd for $C_{17}H_{31}NSiF_4$: C, 57.74; H, 8.86. Found: C, 57.61; H, 8.80.

Preparation of Di-o-tolyldifluorosilane, $(o\text{-Tol})_2SiF_2$. The organofluorosilane had previously been reported by Eaborn[25b] as an impure oil. The compound was prepared as a pure liquid in good yield according to the following modified procedure. Tetrafluorosilane (41.64 g, 400 mmol) was passed through 100 mL of a 2.0 M solution of o-tolylmagnesium chloride (30.18 g, 200 mmol) in THF until refluxing of the ether had ceased (3.5 h). The mixture was refluxed for 4.5 h and then allowed to cool. The mixture was distilled directly to remove THF. The residue was distilled in vacuo to yield a colorless liquid, bp 115–119 °C/2.15 mm. A total of 19.4 g of $(o\text{-Tol})_2SiF_2$ (78% yield) was collected: ^{1}H NMR ($CDCl_3$), 20 °C, 2.43 (s, 6 H, o-Me), 7.18–7.62 (m, 8 H, aromatic ring protons); ^{19}F ($CDCl_3$), 20 °C, −137.9 (d, J_{SiF} = 294 Hz); ^{29}Si NMR ($CDCl_3$), 20 °C, −25.95 (t, J_{SiF} = 293 Hz). Anal. Calcd for $C_{14}H_{14}SiF_2$: C, 67.70; H, 5.69. Found: C, 68.00; H, 5.73.

Preparation of Tetra-o-tolyl-1,3-difluorodisiloxane, $(o\text{-Tol})_2Si(F)OSi(F)(o\text{-Tol})_2$. A solution of $Et_4NF{\cdot}2H_2O$ (4.13 g, 23.3 mmol) was reacted with $o\text{-Tol}_2SiF_2$ (5.53 g, 22.3 mmol) at 25 °C with stirring for 24 h. The solution was concentrated and allowed to cool. Large, colorless crystals formed upon standing. A total of 2.96 g of $(o\text{-Tol})_2Si(F)OSi(F)(o\text{-Tol})_2$ (56% yield) was collected, mp 78–81 °C: ^{1}H ($CDCl_3$) 2.30 (s, o-Me, 12 H), 7.09–7.81 (m, aromatic ring protons, 16 H); ^{19}F ($CDCl_3$) −137.3 (d, J_{SiF} = 283 Hz); ^{29}Si ($CDCl_3$) −34.18 (d, J_{SiF} = 285 Hz). Anal. Calcd for $C_{28}H_{28}Si_2F_2O$: C, 70.84; H, 5.96. Found: C, 70.13; H, 5.89.

X-ray Studies. All X-ray crystallographic studies were done using an Enraf–Nonius CAD4 diffractometer and graphite monochromated molybdenum radiation (λ K$\bar{\alpha}$ = 0.71073 Å) at an ambient temperature of 23 ± 2 °C. Details for the experimental procedures have been described previously.[26]

Crystals were mounted in thin-walled glass capillaries which were sealed as a precaution against moisture sensitivity. Data was collected by using the θ–2θ scan mode with 3° ≤ $2\theta_{MoK\bar{\alpha}}$ ≤ 43° for **1** and **2** and 3° ≤ $2\theta_{MoK\bar{\alpha}}$ ≤ 48° for **3**.

(26) Sau, A. C.; Day, R. O.; Holmes, R. R. *Inorg. Chem.* **1981**, *20*, 3076.

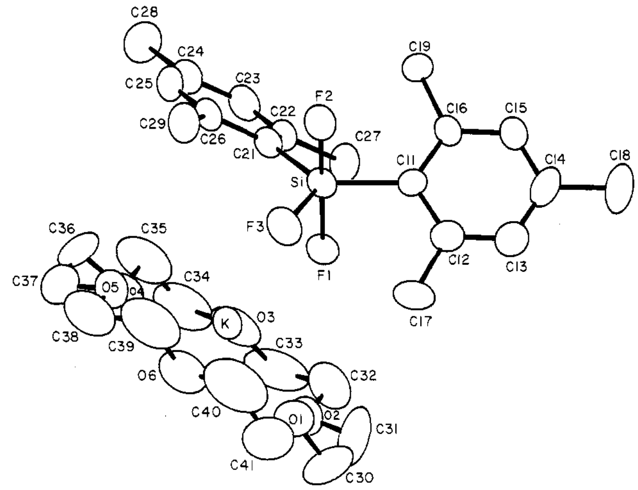

Figure 1. ORTEP plot of the anion and cation in $[Mes_2SiF_3][K,18\text{-}c\text{-}6]{\cdot}CH_2Cl_2$ (**1**) with thermal ellipsoids at the 30% probability level. Hydrogen atoms are omitted for purposes of clarity.

The structures were solved by use of direct methods and difference Fourier techniques and were refined by full-matrix least squares.[27] All computations were performed on a Microvax II computer using the Enraf–Nonius SDP system of programs.

X-ray Crystallographic Study for $[Mes_2SiF_3][K,18\text{-}c\text{-}6]{\cdot}CH_2Cl_2$ (1). The colorless crystal used for the X-ray study was cut from a polycrystalline mass and had dimensions of 0.38 × 0.38 × 0.50 mm.

Crystal Data. $[(C_9H_{11})_2SiF_3][KC_{12}H_{24}O_6]{\cdot}CH_2Cl_2$, monoclinic space group $P2/c$ [C_{2h}^4, no. 13],[28] a = 16.636 (5) Å, b = 15.035 (3) Å, c = 15.720 (4) Å, β = 110.98 (2)°, Z = 4, and $\mu_{MoK\bar{\alpha}}$ = 0.37 mm^{-1}. A total of 4207 independent reflections (+h,+k,±l) was measured. No corrections were made for absorption.

The atoms of the dichloromethane of solvation and several carbon atoms of the cation were poorly defined. However, all of the 44 independent non-hydrogen atoms were refined anisotropically. The 28 independent methylene and aromatic hydrogen atoms were included in the refinement as isotropic scatterers in idealized positions riding on the bonded carbon atoms. Methyl hydrogen atoms were omitted from the refinement. The final agreement factors[29] were R = 0.088 and R_w = 0.113 for the 2362 reflections having $I \geq 3\sigma_I$.

X-ray Crystallographic Study for $[Mes_2Si(F)O]_2[H][Et_4N]$ (2). The colorless crystal used for the X-ray study was cut from a fused mass of rectangular plate-like crystals and had dimensions of 0.10 × 0.28 × 0.34 mm.

Crystal Data. $[(C_9H_{11})_2Si(F)O]_2[H][Et_4N]$, monoclinic space group $P2_1/n$, alternate setting of $P2_1/c$ [C_{2h}^5, no. 14],[30] a = 8.567 (2) Å, b = 9.479 (3) Å, c = 26.754 (5) Å, β = 96.06 (2)°, Z = 2, and $\mu_{MoK\bar{\alpha}}$ = 0.12 mm^{-1}. A total of 2480 independent reflections (+h,+k,±l) was measured. No corrections were made for absorption.

All non-hydrogen atoms were refined anisotropically. The nitrogen atom of the tetraethylammonium ion lies on an inversion center with the terminal carbon of the ethyl groups (C24, C25) conforming to the C_i symmetry. The four methylene carbon atoms (C20–C23) are disordered about the inversion center and were included in the refinement with half occupancy. The 22 independent hydrogen atoms of the mesitylene groups were included in the refinement as isotropic scatterers riding on the carbon atoms (methyl hydrogen atoms regularized from difference Fourier locations, aromatic hydrogen atoms in ideal positions). The hydrogen atoms of the disordered cation were omitted from the refinement. The final agreement factors were R = 0.065 and R_w = 0.087 for the 1253 reflections having $I \geq 2\sigma_I$. A final difference Fourier synthesis showed a maximum density of 0.32 ± 0.06 e/Å^3 at the inversion center located between the oxygen atoms.

X-ray Crystallographic Study for $(Mes_2SiF)_2O$ (3). The colorless crystal used for the X-ray study was an irregular lump cut from a polycrystalline mass with maximum dimensions of 0.33 × 0.33 × 0.40 mm.

Crystal Data. $((C_9H_{11})_2SiF)_2O$, monoclinic space group $C2/c$, a = 14.337 (2) Å, b = 12.458 (4) Å, c = 18.577 (4) Å, β = 92.31 (1)°, Z

(27) The function minimized was $\sum w(|F_o| - |F_c|)^2$, where $w^{1/2} = 2F_oLp/\sigma_I$.

(28) *International Tables for X-ray Crystallography*; Kynoch: Birmingham, England, 1969; Vol. I, p 97.

(29) $R = \sum||F_o| - |F_c||/\sum|F_o|$ and $R_w = \{\sum w(|F_o| - |F_c|)^2/\sum w|F_o|^2\}^{1/2}$.

(30) Reference 28, p 99.

Table II. Atomic Coordinates in Crystalline $[Mes_2SiF_3][K,18\text{-}c\text{-}6]\cdot CH_2Cl_2$, **1**[a]

atom[b]	x	y	z	B equiv[c]	atom[b]	x	y	z	B equiv[c]
K	0.1961 (1)	0.2263 (2)	0.6156 (1)	5.95 (6)	C23	0.3494 (6)	0.5332 (7)	0.7522 (6)	6.5 (3)
Si	0.2641 (2)	0.3072 (2)	0.8526 (2)	5.11 (7)	C24	0.2772 (6)	0.5893 (7)	0.7200 (6)	6.9 (3)
F1	0.3020 (3)	0.2550 (3)	0.7765 (3)	6.2 (1)	C25	0.2021 (6)	0.5596 (7)	0.7264 (6)	6.2 (3)
F2	0.2216 (3)	0.3516 (4)	0.9250 (3)	6.2 (1)	C26	0.1956 (5)	0.4765 (7)	0.7651 (5)	5.7 (3)
F3	0.1737 (3)	0.2531 (4)	0.8025 (4)	7.7 (2)	C27	0.4308 (5)	0.3961 (7)	0.8182 (6)	6.5 (3)
O1	0.1923 (6)	0.0422 (5)	0.6427 (5)	10.0 (3)	C28	0.2821 (8)	0.6824 (7)	0.6756 (7)	9.2 (4)
O2	0.3265 (5)	0.1058 (6)	0.5934 (5)	9.5 (2)	C29	0.1069 (5)	0.4467 (7)	0.7651 (6)	7.0 (3)
O3	0.3282 (5)	0.2869 (6)	0.5563 (5)	10.5 (2)	C30	0.2534 (9)	−0.0155 (8)	0.6257 (8)	13.0 (5)
O4	0.1713 (6)	0.3714 (5)	0.4882 (5)	10.9 (3)	C31	0.3352 (9)	0.032 (1)	0.6486 (8)	14.5 (5)
O5	0.0340 (5)	0.3089 (6)	0.5433 (5)	11.0 (3)	C32	0.3997 (8)	0.152 (1)	0.6187 (9)	13.9 (5)
O6	0.0350 (5)	0.1350 (6)	0.5869 (5)	10.4 (3)	C33	0.3918 (7)	0.228 (1)	0.5514 (9)	15.0 (5)
C11	0.3535 (5)	0.2513 (5)	0.9511 (5)	4.5 (2)	C34	0.3150 (9)	0.3628 (9)	0.4950 (9)	14.0 (5)
C12	0.3640 (6)	0.1583 (6)	0.9559 (6)	6.0 (3)	C35	0.245 (1)	0.4199 (9)	0.5094 (9)	15.7 (5)
C13	0.4295 (6)	0.1157 (7)	1.0222 (6)	6.6 (3)	C36	0.095 (1)	0.4250 (7)	0.4906 (9)	14.7 (5)
C14	0.4863 (6)	0.1650 (6)	1.0912 (6)	6.6 (3)	C37	0.0201 (9)	0.3662 (9)	0.472 (1)	13.6 (5)
C15	0.4783 (6)	0.2567 (6)	1.0911 (6)	6.1 (3)	C38	−0.0446 (8)	0.264 (1)	0.529 (1)	15.0 (6)
C16	0.4116 (5)	0.2997 (6)	1.0235 (5)	4.7 (2)	C39	−0.0222 (7)	0.194 (1)	0.6066 (9)	15.0 (5)
C17	0.2976 (8)	0.0948 (7)	0.8863 (7)	8.8 (4)	C40	0.0543 (9)	0.069 (1)	0.6499 (9)	16.2 (5)
C18	0.5634 (8)	0.1202 (8)	1.1682 (8)	10.4 (4)	C41	0.111 (1)	0.0049 (9)	0.627 (1)	15.3 (6)
C19	0.4064 (6)	0.4021 (6)	1.0307 (6)	6.4 (3)	C11	0.1036 (5)	0.1250 (5)	0.4063 (4)	24.1 (3)
C21	0.2694 (5)	0.4173 (6)	0.7993 (5)	4.7 (2)	C12	0.1506 (7)	0.2046 (7)	0.2848 (6)	43.1 (5)
C22	0.3460 (5)	0.4499 (6)	0.7895 (5)	5.0 (2)	C1	0.1831 (9)	0.135 (1)	0.370 (1)	19.3 (7)

[a] Numbers in parentheses are estimated standard deviations. [b] Atoms are labeled to agree with Figure 1. [c] Equivalent isotropic thermal parameters are calculated as $(^4/_3)[a^2\beta_{11} + b^2\beta_{22} + c^2\beta_{33} + ab(\cos\gamma)\beta_{12} + ac(\cos\beta)\beta_{13} + bc(\cos\alpha)\beta_{23}]$.

Table III. Selected Distances (Å) and Angles (deg) for $[Mes_2SiF_3][K,18\text{-}c\text{-}6]\cdot CH_2Cl_2$, **1**[a]

atom 1	atom 2	distance	atom 1	atom 2	distance	atom 1	atom 2	distance
Si	F1	1.729 (6)	Si	C21	1.872 (9)	K	O3	2.828 (9)
Si	F2	1.678 (6)	K	F1	2.549 (4)	K	O4	2.890 (8)
Si	F3	1.641 (6)	K	O1	2.804 (8)	K	O5	2.812 (8)
Si	C11	1.915 (7)	K	O2	2.942 (9)	K	O6	2.898 (8)

atom 1	atom 2	atom 3	angle	atom 1	atom 2	atom 3	angle
F1	Si	F2	175.6 (3)	F2	Si	C11	91.2 (3)
F1	Si	F3	86.6 (3)	F2	Si	C21	93.0 (4)
F1	Si	C11	89.4 (3)	F3	Si	C11	118.9 (4)
F1	Si	C21	90.2 (3)	F3	Si	C21	113.9 (3)
F2	Si	F3	89.3 (3)	C11	Si	C21	127.0 (4)

[a] Estimated standard deviations in parentheses. The atom labeling scheme is shown in Figure 1.

Table IV. Atomic Coordinates in Crystalline $[Mes_2Si(F)O]_2[H][Et_4N]$, **2**[a]

atom[b]	x	y	z	B equiv[c]	atom[b]	x	y	z	B equiv[c]
Si	0.9967 (3)	0.0250 (3)	0.40845 (9)	4.16 (6)	C12	0.6964 (9)	0.1705 (9)	0.4107 (3)	4.1 (2)
F1	1.1482 (6)	0.1309 (5)	0.4156 (2)	6.5 (1)	C13	0.582 (1)	0.2720 (9)	0.3924 (4)	5.8 (3)
O	0.9839 (7)	−0.0559 (6)	0.4588 (2)	5.5 (2)	C14	0.602 (1)	0.356 (1)	0.3523 (4)	6.2 (3)
N	0.500[d]	0.000[d]	0.000[d]	6.5 (3)	C15	0.738 (1)	0.3410 (9)	0.3295 (3)	5.7 (3)
C1	1.0337 (9)	−0.1042 (8)	0.3573 (3)	3.2 (2)	C16	0.851 (1)	0.2422 (9)	0.3454 (3)	4.9 (2)
C2	1.1874 (9)	−0.1417 (8)	0.3481 (3)	3.5 (2)	C17	0.663 (1)	0.084 (1)	0.4561 (3)	6.2 (3)
C3	1.212 (1)	−0.2361 (8)	0.3091 (3)	4.0 (2)	C18	0.479 (1)	0.462 (1)	0.3342 (4)	9.2 (3)
C4	1.088 (1)	−0.2969 (8)	0.2802 (3)	4.1 (2)	C19	0.992 (1)	0.231 (1)	0.3150 (3)	7.3 (3)
C5	0.938 (1)	−0.2655 (9)	0.2902 (3)	4.3 (2)	C20	0.500 (3)	0.060 (2)	−0.0543 (7)	8.4 (7)
C6	0.9110 (9)	−0.1718 (8)	0.3278 (3)	3.9 (2)	C21	0.418 (3)	−0.149 (2)	−0.0036 (9)	8.4 (7)
C7	1.3316 (9)	−0.0890 (9)	0.3798 (3)	5.6 (3)	C22	0.395 (3)	0.103 (2)	0.0265 (9)	9.7 (8)
C8	1.119 (1)	−0.399 (1)	0.2383 (3)	6.6 (3)	C23	0.668 (3)	−0.022 (3)	0.0279 (9)	11.8 (8)
C9	0.7383 (9)	−0.144 (1)	0.3351 (4)	6.6 (3)	C24	0.613 (2)	−0.047 (2)	−0.0833 (4)	13.7 (5)
C11	0.8345 (9)	0.1533 (8)	0.3874 (3)	3.6 (2)	C25	0.758 (2)	0.132 (1)	0.0312 (6)	12.4 (5)

[a] Numbers in parentheses are estimated standard deviations. [b] Atoms are labeled to agree with Figure 2. [c] Equivalent isotropic thermal parameters are calculated as $(^4/_3)[a^2\beta_{11} + b^2\beta_{22} + c^2\beta_{33} + ab(\cos\gamma)\beta_{12} + ac(\cos\beta)\beta_{13} + bc(\cos\alpha)\beta_{23}]$. [d] Fixed.

= 4, and $\mu_{MoK\bar{\alpha}}$ = 0.14 mm^{-1}. A total of 2608 independent reflections ($+h,+k,\pm l$) was measured. No corrections were made for absorption.

The 21 independent non-hydrogen atoms were refined anisotropically. The 22 independent hydrogen atoms were treated as described for **2**. The final agreement factors were R = 0.048 and R_w = 0.057 for the 1624 reflections having $I \geq 2\sigma_I$.

Results

The atom labeling scheme for **1** is given in the ORTEP plot of Figure 1. Atomic coordinates are given in Table II, while selected bond lengths and angles are given in Table III. The corresponding information for **2** and **3** is given in Figures 2 and 3 and in Tables IV–VII. Thermal parameters, hydrogen atom parameters, and

Table V. Selected Distances (Å) and Angles (deg) for $[Mes_2Si(F)O]_2[H][Et_4N]$, **2**[a]

atom 1	atom 2	distance	atom 1	atom 2	distance
Si	F1	1.636 (5)	Si	O	1.565 (6)
Si	C1	1.888 (8)	O	O′	2.434 (7)
Si	C11	1.887 (8)			

atom 1	atom 2	atom 3	angle	atom 1	atom 2	atom 3	angle
F1	Si	O	109.1 (3)	O	Si	C11	117.1 (4)
F1	Si	C1	106.9 (3)	C1	Si	C11	112.1 (3)
F1	Si	C11	100.9 (3)	Si	O	O′	123.7 (3)
O	Si	C1	109.8 (3)				

[a] Estimated standard deviations in parentheses. The atom labeling scheme is shown in Figure 2.

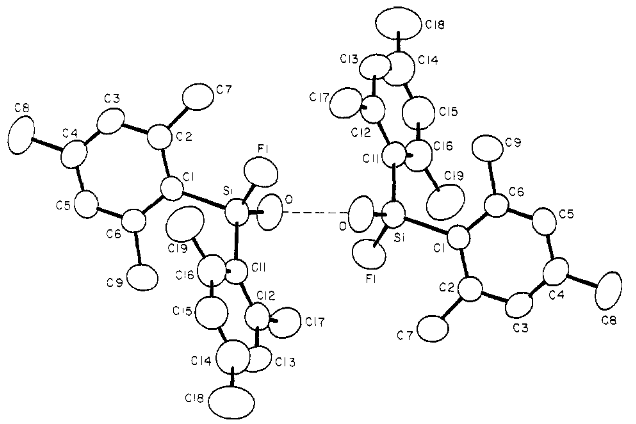

Figure 2. ORTEP plot of the anion in $[Mes_2Si(F)O]_2[H][Et_4N]$ (**2**) with thermal ellipsoids at the 30% probability level. Atoms on the right of the figure are inversion related $(2 - x, -y, 1 - z)$ to those on the left with the same label. The interaction of the oxygen atoms with the proton is indicated by a dashed line. Hydrogen atoms are omitted for purposes of clarity.

Table VI. Atomic Coordinates in Crystalline $(Mes_2SiF)_2O$, **3**[a]

atom[b]	x	y	z	B equiv[c]
Si	0.40389 (6)	0.21913 (7)	0.70667 (5)	4.70 (2)
F	0.3258 (1)	0.1976 (1)	0.7637 (1)	6.18 (5)
O	0.500[d]	0.1864 (2)	0.750[d]	4.98 (7)
C1	0.3727 (2)	0.1265 (2)	0.6304 (2)	4.72 (7)
C2	0.4266 (2)	0.0379 (3)	0.6087 (2)	4.92 (7)
C3	0.3923 (3)	−0.0295 (3)	0.5540 (2)	6.01 (9)
C4	0.3067 (3)	−0.0154 (3)	0.5201 (2)	6.64 (9)
C5	0.2547 (2)	0.0714 (3)	0.5400 (2)	6.65 (9)
C6	0.2852 (2)	0.1423 (3)	0.5941 (2)	5.65 (8)
C7	0.5222 (2)	0.0102 (3)	0.6416 (2)	6.47 (9)
C8	0.2688 (3)	−0.0930 (4)	0.4628 (2)	10.0 (1)
C9	0.2211 (2)	0.2359 (3)	0.6130 (2)	7.5 (1)
C11	0.4081 (2)	0.3650 (3)	0.6846 (2)	4.94 (7)
C12	0.3589 (2)	0.4451 (3)	0.7203 (2)	5.59 (8)
C13	0.3748 (2)	0.5531 (3)	0.7049 (2)	6.26 (9)
C14	0.4354 (2)	0.5851 (3)	0.6544 (2)	6.22 (9)
C15	0.4818 (2)	0.5069 (3)	0.6173 (2)	6.23 (9)
C16	0.4688 (2)	0.3988 (3)	0.6310 (2)	5.20 (8)
C17	0.2874 (3)	0.4218 (3)	0.7772 (2)	8.4 (1)
C18	0.4505 (3)	0.7040 (3)	0.6399 (3)	9.3 (1)
C19	0.5226 (3)	0.3188 (3)	0.5868 (2)	6.97 (9)

[a] Numbers in parentheses are estimated standard deviations. [b] Atoms are labeled to agree with Figure 3. [c] Equivalent isotropic thermal parameters are calculated as $(^4/_3)[a^2\beta_{11} + b^2\beta_{22} + c^2\beta_{33} + ab(\cos\gamma)\beta_{12} + ac(\cos\beta)\beta_{13} + bc(\cos\alpha)\beta_{23}]$.

Table VII. Selected Distances (Å) and Angles (deg) for $(Mes_2SiF)_2O$, **3**[a]

atom 1	atom 2	distance	atom 1	atom 2	distance
Si	F	1.595 (2)	Si	C1	1.867 (3)
Si	O	1.620 (1)	Si	C11	1.865 (3)

atom 1	atom 2	atom 3	angle	atom 1	atom 2	atom 3	angle
F	Si	O	103.5 (1)	O	Si	C11	108.7 (1)
F	Si	C1	104.3 (1)	C1	Si	C11	116.4 (1)
F	Si	C11	109.9 (1)	Si	O	Si′	150.8 (2)
O	Si	C1	113.2 (1)				

[a] Estimated standard deviations in parentheses. The atom labeling scheme is shown in Figure 3.

additional bond lengths and angles for all three compounds are provided as Supplementary Material.

Discussion

As noted in the introduction, dimesityldifluorosilane does not react with water even under extended reflux in acetonitrile. However, as Figure 4 illustrates, a complex ^{19}F NMR spectrum results when tetraethylammonium fluoride dihydrate and dimesityldifluorosilane are reacted in acetonitrile in the presence of the water scavenger, dimethoxypropane. The ^{19}F spectrum is for a $CDCl_3$ solution of the precipitate which formed within a few

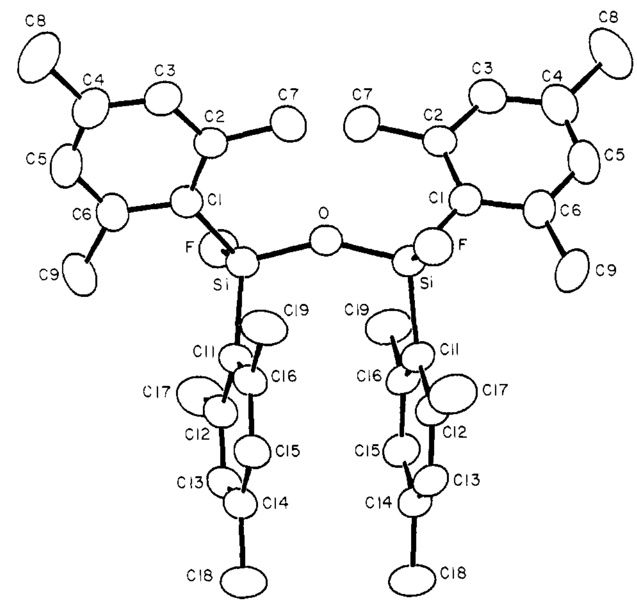

Figure 3. ORTEP plot of $(Mes_2SiF)_2O$ (**3**) with thermal ellipsoids at the 30% probability level. Atoms on the right of the figure are 2-fold related $(1 - x, y, 1.5 - z)$ to those on the left with the same label. The oxygen atom lies on the 2-fold axis. Hydrogen atoms are omitted for purposes of clarity.

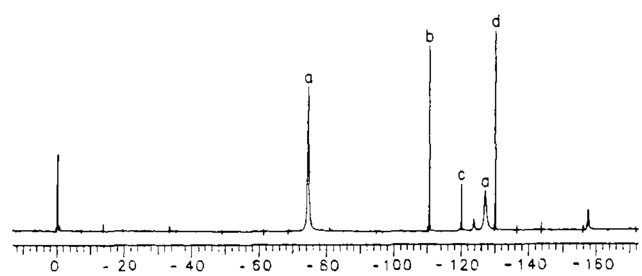

Figure 4. ^{19}F NMR spectrum of a $CDCl_3$ solution of the reaction product of Mes_2SiF_2 with $Et_4NF{\cdot}2H_2O$ in the presence of DMP in acetonitrile solution. The products formed at 25 °C are (a) $[Mes_2SiF_3]^-$ (F_{ax}), (b) $[MesSiF_4]^-$, (c) $Mes_2Si(F)$-O-$Si(F)Mes_2$, (a) $[Mes_2SiF_3]^-$ (F_{eq}), and (d) $[Mes_2Si(F)O$-H-$OSi(F)Mes_2]^-$. The small signal at −123.8 ppm is due to unreacted Mes_2SiF_2, while the small signal at −157.6 ppm is unassigned.

minutes of the reaction conducted at room temperature. Subsequent work outlined in the Experimental Section led to the identification of the peaks labeled a–d. This was achieved by isolation of the various components and by independently synthesizing each one.

The low and high field peaks labeled a are ^{19}F signals from the axial and equatorial fluorine atoms of the trigonal bipyramidal anion, $Mes_2SiF_3^-$, which is nonexchanging at room temperature. This substance, $[Mes_2SiF_3][Et_4N]$, formed from the reaction mixture described above by selective crystallization (see isolation of the bisilonate **2** in the Experimental Section). The first crystals isolated were that due to $(Mes_2SiF)_2O$ (**3**), peak c, insoluble in acetonitrile. On further concentration of the filtrate, crystalline $[Mes_2SiF_3][Et_4N]$ formed. Finally, recrystallization of the latter gave the hydrogen bisilonate $[Mes_2Si(F)O]_2[H][Et_4N]$ (**2**), peak d in Figure 4.

Since the dimesityltrifluorosilicate anion as the tetraethylammonium salt readily hydrolyzes in the presence of trace amounts of water, the KF·18-crown-6 complex was prepared for further characterization and X-ray analysis. The dimesityltrifluorosilicate anion was prepared in toluene solution both as a methylene chloride solvate, $[Mes_2SiF_3][K,18\text{-}c\text{-}6]{\cdot}CH_2Cl_2$ (**1**), used for the X-ray determination, and as the unsolvated complex, eq 2.

$$Mes_2SiF_2 + KF + 18\text{-}c\text{-}6 \xrightarrow[25\ ^\circ C]{toluene} [Mes_2SiF_3][K,18\text{-}c\text{-}6] \quad (2)$$

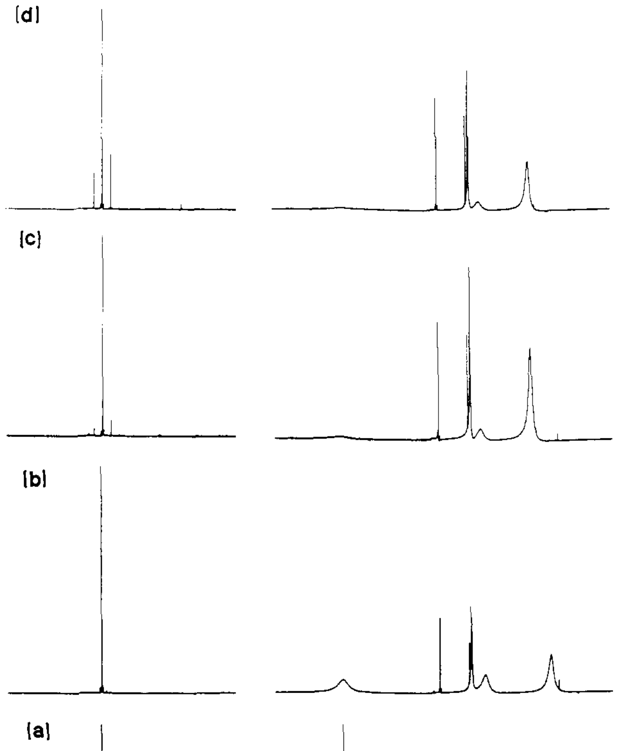

Figure 5. The left side shows ^{19}F NMR spectra at 25 °C of (a) an acetone solution of Mes_2SiF_2; (b) the solution in (a) to which water was added to give a 2:1 molar ratio of water to Mes_2SiF_2 recorded after 5 min of mixing; (c) the solution of (b) after 15 min, and (d) the solution in (b) after 24 h. The right side shows an identical time sequence and molar solution concentrations of the ^{19}F NMR spectra at 25 °C of an acetone solution of $[Mes_2SiF_3][K,18\text{-}c\text{-}6]$. Proceeding from low to high field, the ^{19}F signals in (b)–(d) arise from $[Mes_2SiF_3]^-$ (F_{ax}) at −76.04 ppm, $[MesSiF_4]^-$ at −109.26 ppm, $[Mes_2Si(F)O\text{-}H\text{-}OSi(F)Mes_2]^-$ at −119.24 ppm, $Mes_2Si(F)\text{-}O\text{-}Si(F)Mes_2$ at −120.1 ppm, $[Mes_2SiF_3]^-$ (F_{eq}) at −125.81 ppm, and an unidentified peak which varies between −148 and −140 ppm.

In a quantitative experiment described in the Experimental Section, the ^{19}F NMR spectra illustrating the relative rates of hydrolysis of Mes_2SiF_2 and $[Mes_2SiF_3][K,18\text{-}c\text{-}6]$ at 20 °C were obtained. The spectra are shown in Figure 5. It is apparent that no significant change occurs over a 24 h period for the ^{19}F signal associated with Mes_2SiF_2 in contact with excess water in acetone. In contrast, extensive hydrolytic reaction of the pentacoordinate anionic silicate has taken place within 5 min under similar conditions. Reaction is essentially complete after 15 min as indicated by the lack of significant spectral changes between this period and after 24 h. Further, varying the ratio of water to silicon reactant over the range from a 1:1 to a 10:1 molar ratio did not reveal any concentration dependence. The products observed are the same ones identified in the ^{19}F NMR spectrum formed from the reaction of Mes_2SiF_2 with $Et_4NF{\cdot}2H_2O$ (Figure 4). Hence, it seems clear that the formation of the $Mes_2SiF_3^-$ anion is the intermediate responsible for the acceleration in hydrolysis occurring in the latter case. These results agree with rate enhancement effects Corriu et al.[21a] and Sakurai et al.[21b,c] described supporting an enhanced reactivity for five-coordinated acyclic silicates.

The hydrogen bisilonate **2** and disiloxane **3** that formed in the product mixture and contributed to the NMR spectrum in Figure 4 obviously are hydrolysis products. The disiloxane **3** may be obtained in relatively high yields, both from the treatment of $[Mes_2SiF_3][K,18\text{-}c\text{-}6]$ with water (62%) and from the reaction of Mes_2SiF_2 with $Et_4NF{\cdot}2H_2O$ in the absence of DMP (71%). In a related reaction, hydrolysis of di-*o*-tolyldifluorosilane yielded the difluorodisiloxane, $(o\text{-}Tol)_2Si(F)\text{-}O\text{-}Si(F)(o\text{-}Tol)_2$.

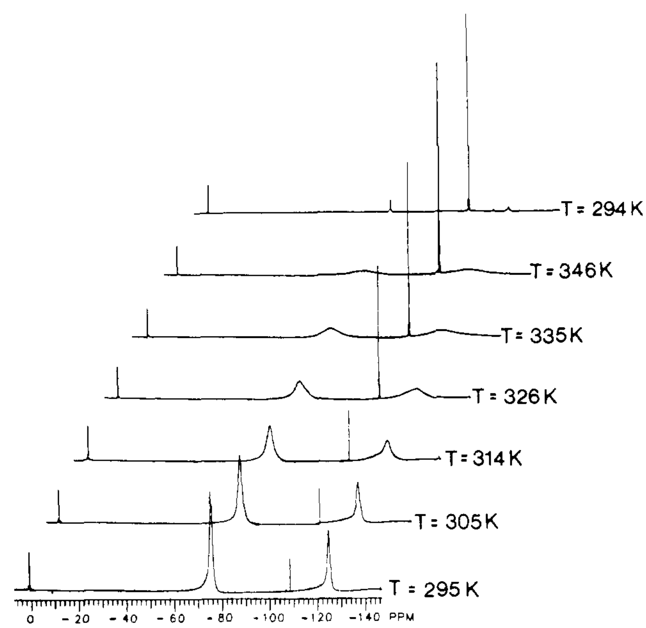

Figure 6. ^{19}F NMR spectrum of $[Mes_2SiF_3][K,18\text{-}c\text{-}6]$ in CD_3CN solution illustrating the onset of fluorine atom exchange (broadening of peaks at −76.2 and −124.2 ppm) accompanying the irreversible formation of $MesSiF_4^-$ (peak at −108.3 ppm) as the temperature is increased.

An indication of the complexity of the hydrolysis process leading to the disiloxane **3** from the K,18-c-6 salt of $Mes_2SiF_3^-$ is found on examination of the ^{19}F NMR spectrum of the latter substance in CD_3CN as a function of temperature (Figure 6). As the temperature is increased above room temperature, broadening occurs for the signals associated with the axial and equatorial fluorine atoms of $Mes_2SiF_3^-$, indicative of the onset of rapid ligand exchange. Accompanying this change, a new sharp peak appears at −108.3 ppm increasing in intensity as further broadening and disappearance of the axial and equatorial fluorine atom signals continues. The process nears completion at 48 °C and is shown to be irreversible on cooling the sample to room temperature. The new ^{19}F signal corresponds to peak b in Figure 4. Independent synthesis from Mes_2SiF_2 and $Et_4NF{\cdot}2H_O$ in refluxing acetonitrile and characterization identifies peak b as the fluorine resonance for $[Et_4N][MesSiF_4]$ (**4**) undergoing rapid ligand exchange. Since ^{29}Si satellites are present, the exchange is intramolecular.

These results suggest a common hydrolysis reaction for the formation of the disiloxane **3** and the $MesSiF_4^-$ anion from hydrolysis of the $Mes_2SiF_3^-$ anion and from the interaction of Mes_2SiF_2 with $Et_4NF{\cdot}2H_2O$. Formation of $MesSiF_4^-$ involves Si–C bond cleavage and indicates the formation of mesitylene. A hydrolysis pathway taking these considerations into account is given in eq 3. Since Mes_2SiF_2 does not react with water, interaction of Mes_2SiF_2 with $Et_4NF{\cdot}2H_2O$ is expected to first form the pentacoordinated anion, $Mes_2SiF_3^-$, followed by hydrolysis as expressed in eq 3.

$$4Mes_2SiF_3^- + H_2O \xrightarrow{CH_3CN} 2MesSiF_4^- + 2MesH + Mes_2Si(F)\text{-}O\text{-}Si(F)Mes_2 + 2F^- \quad (3)$$

It is possible that the hydrolysis in the NMR tube resulting in the spectrum in Figure 5 is more complicated. Although, $(Mes_2SiF)_2O$ (**3**) is insoluble in CH_3CN and hence does not contribute a ^{19}F signal, sufficient water must be present for the process in eq 3 to go to completion. A competing reaction of $Mes_2SiF_3^-$ with adventitious water might yield HF, eq 4. Attack on glass then would generate additional water for the hydrolysis.

However, further work is needed to clarify this point.

$$2Mes_2SiF_3^- + H_2O \xrightarrow{CD_3CN} Mes_2Si(F)\text{-}O\text{-}Si(F)Mes_2 + 2HF + 2F^- \quad (4)$$

Formation of the disiloxane **3** also readily occurs by exposing the hydrogen bisilonate **2** to atmospheric moisture or wet acetonitrile, eq 5. The disiloxane **3** itself is stable to further hydrolysis.

$$[Mes_2Si(F)O\text{-}H\text{-}OSi(F)Mes_2][Et_4N] \rightarrow Mes_2Si(F)\text{-}O\text{-}Si(F)Mes_2 + Et_4NOH \quad (5)$$

The isolation of small amounts of the hydrogen bisilonate **2** was achieved only on recrystallization of $[Mes_2SiF_3][Et_4N]$. The latter was formed in the reaction of Mes_2SiF_2 with $Et_4NF{\cdot}2H_2O$ in acetonitrile in the presence of DMP. One can write the following expression for the hydrolysis leading to the hydrogen bisilonate **2**, eq 6. This is somewhat analogous to the hydrolysis written for the formation of the disiloxane **3** from the $Mes_2SiF_3^-$ anion in eq 4.

$$2[Mes_2SiF_3][Et_4N] + 2H_2O \xrightarrow{CH_3CN} [Mes_2Si(F)O\text{-}H\text{-}OSi(F)Mes_2][Et_4N] + [Et_4N][HF_2] + 2HF \quad (6)$$

As the section on Structural Details outlines, X-ray analysis of **1–3** shows that the $Mes_2SiF_3^-$ anion has the expected trigonal bipyramidal geometry, analogous to that of related isoelectronic phosphoranes, R_2PF_3. The disiloxane **3** has the expected ether structure. However, the hydrogen bisilonate **2** exhibits a unique structure in which hydrogen bonding apparently holds two $Mes_2Si(F)O$ units together.

Mechanistically, this rather elusive substance may be viewed as a model for a likely intermediate in the first stages of silicic acid polymerization as a precursor to the formation of the disiloxane, $(HO)_3Si\text{-}O\text{-}Si(OH)_3$, in the sol-gel process.[22] It is probable that isolation of the hydrogen bisilonate **2** in *this* work relates to the use of the rather sizeable mesityl substituents which act as protecting groups to increase its stability toward hydrolysis sufficiently to allow detection. This is not to say that all possible stages in the hydrolytic sequence, Mes_2SiF_2, $Mes_2SiF_3^-$, $Mes_2Si(F)O\text{-}H\text{-}OSi(F)Mes_2^-$, $Mes_2Si(F)\text{-}O\text{-}Si(F)Mes_2$, have been isolated even though we have performed a careful search. For example, we found no evidence for the presence of $Mes_2Si(OH)F$ or $Mes_2Si(OH)_2$ under the mild conditions for the reactions of concern in Figures 4 and 5. We have, however, isolated and characterized $Mes_2Si(OH)F$ from refluxing methanol.[31] It exhibited a characteristic OH stretching frequency at 3410 cm^{-1}. The latter allowed it to be differentiated from $(Mes_2SiF)_2O$ which had similar NMR properties. In any event, the rapid hydrolysis reaction we observe suggests that species analogous to the pentacoordinated anionic silicate, $Mes_2SiF_3^-$, and the anionic hydrogen bisilonate, $Mes_2Si(F)O\text{-}H\text{-}OSi(F)Mes_2$, may appear as intermediates in the sol-gel process.

On the basis of *this* study, therefore, a plausible model suggested for the initial reactions in the hydrolysis of silicic acid, $Si(OH)_4$, is shown in Scheme I. In this scheme, one has an experimental basis for proposing the hydrogen bonded intermediate C. D is a rearrangement form of C in which the hydroxyl group involved in the hydrogen-bonded portion of C assumes a trans axial position of an emerging trigonal bipyramid formed as the two silicon atoms move closer to one another. D may be formally viewed as an axial attack of the $(HO)_3SiO^-$ group on a silicic acid molecule. Since we have found that a five-coordinated anionic silicate is necessary for hydrolysis of Mes_2SiF_2 to occur, in an analogous fashion, the formation of A, $Si(OH)_5^-$, is proposed in agreement with previous suggestions.[32] B then is a likely intermediate, formed from interaction of A with $Si(OH)_4$, on the way to the hydrogen bisilonate, C. Forms B and D, each of which contains four- and five-coordinated silicon atoms, may be more likened to a transition state than an intermediate.

If step **2** is rate limiting, second-order kinetics in silicon is realized in agreement with that found for base catalysis.[22c] In acid media, below pH 2, where reaction is slower, if step **4** becomes competitive, perhaps because of the reduced concentration of D $[Si(OH_3)O^- + H^+ \rightarrow Si(OH)_4]$, a third-order rate law may be obeyed, as found.[22c] The regeneration of the catalyst, $Si(OH)_5^-$, in the last step causes the cycle to repeat by a greater number of possible pathways.

To examine the feasibility of this mechanistic route in terms of the energetics involved, ab initio calculations were performed. For each species in the proposed reaction mechanism, the structure was optimized with GAUSSIAN 86[33] with a minimal basis set,

Scheme I

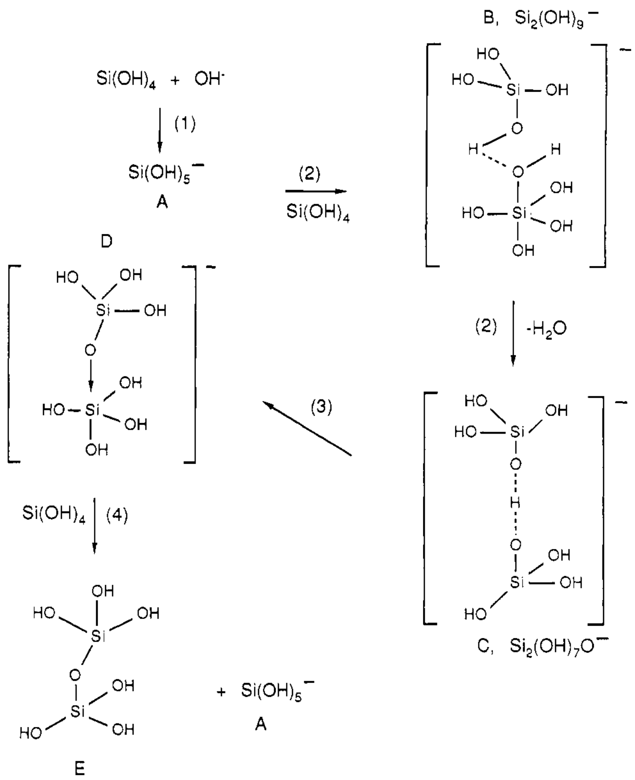

Table VIII. Calculated Energy, E(RHF), for Reactants and Products in Scheme I for Silanol Polymerization, au

	STO-3G	6-31+G*
$[OH]^-$	−74.065017	−75.376424
H_2O	−74.965901	−76.017743
$Si(OH)_4$	−583.372002	−590.898898
$[Si(OH)_5]^-$	−657.649991	−666.372450
$[(OH)_3SiOHOSi(OH)_3]^-$	−1166.036576	−1181.263481[a]
$[(OH)_3SiOSi(OH)_4]^-$	−1166.095162	b
$(OH)_3SiOSi(OH)_3$	−1091.786311	−1105.784602[a]

[a] Single-point calculation based on geometry optimized at STO-3G. [b] Since this species has no symmetry, the memory requirement for a single-point calculation was prohibitively large.

(31) Under more forcing conditions, hydrolysis of $(t\text{-}Bu)_2SiF_2$ in refluxing dimethyl sulfoxide for 20 h gave a 25% yield of $(t\text{-}Bu)_2Si(F)OH$ and a 16% yield of $(t\text{-}Bu)_2Si(OH)_2$: Buttrus, N. H.; Eaborn, C.; Hitchcock, P. B.; Saxena, A. K. *J. Organomet. Chem.* **1985**, *284*, 291; **1985**, *287*, 157.

(32) (a) Reference 22a, Chapter 3. (b) Davis, L. P.; Burggraf, L. W. Application of MNDO to Silicon Chemistry. In *Science of Ceramic Chemical Processing*; Hench, L. L., Ulrich, D. R., Eds.; John Wiley and Sons: New York, 1986; pp 400–411. (c) Davis, L. P.; Burggraf, L. W. *A Theoretical Study of the Silanol Polymerization Mechanism*; Third International Conference on Ultrastructure Processing of Ceramics, Glasses, and Composites, San Diego, CA, February 23–27, 1987; Paper 28.

(33) GAUSSIAN 86: Frisch, M. J.; Binkley, J. S.; Schlegel, H. B.; Raghavachari, K.; Melius, C. F.; Martin, R. L.; Stewart, J. J. P.; Bobrowicz, F. W.; Rohlfing, C. M.; Kahn, L. R.; Defrees, D. J.; Seeger, R.; Whiteside, R. A.; Fox, D. J.; Fleuder, E. M.; Pople, J. A. Carnegie-Mellon Quantum Chemistry Publishing Unit: Pittsburgh, PA, 1984.

Table IX. Energetics of Proposed Reaction Mechanism in Scheme I for Silanol Polymerization, kcal/mol

	STO-3G	6-31+G*
reaction step[a]		
1	−133.63	−60.94
2	12.25	−6.20
3	−36.76	b
4	+19.36	b
overall reaction	−138.78	−63.80

[a] Step 1: $Si(OH)_4 + OH^- \rightarrow [Si(OH)_5]^-$. Step 2: $Si(OH)_4 + Si(OH)_5^- \rightarrow [(OH)_3Si\text{-}O\text{-}H\text{-}O\text{-}Si(OH)_3]^- + H_2O$. Step 3: $[(OH)_3SiOHOSi(OH)_3]^- \rightarrow [(OH)_4Si\text{-}O\text{-}Si(OH)_3]^-$. Step 4: $[(OH)_4Si\text{-}O\text{-}Si(OH)_3]^- + Si(OH)_4 \rightarrow [Si(OH)_5]^- + (OH)_3Si\text{-}O\text{-}Si(OH)_3$. Overall reaction: $3Si(OH)_4 + OH^- \rightarrow H_2O + Si(OH)_5^- + (OH)_3SiOSi(OH)_3$. [b] The energy change for the combined steps 3 and 4 is 3.34 kcal/mol.

STO-3G, and a larger basis set, 6-31+G*. The minimum energies for each of these calculations are shown in Table VIII. For the larger species with more than one silicon atom, a single-point calculation at STO-3G geometry was done with the 6-31+G* basis set since optimization of these larger species at the 6-31+G* level was not feasible. Throughout the optimization, the Si–OH bond angle and OH bond length for the hydroxide moieties (i.e., not involved in the reaction site) were fixed at 106.9° and 0.96 Å, respectively.

The energy changes associated with each stage of the reaction pathway are shown in Table IX. It is seen that the initial step has the greatest release of energy, while the other steps show smaller energy changes, none of which indicate a high-energy state. On this basis, the mechanism proposed in Scheme I represents a feasible pathway of low energy. Both the relative stability of the five-coordinated anionic silicate, $Si(OH)_5^-$, and that of the hydrogen-bonded bisilonate, $(HO)_3Si\text{-}O\text{-}H\text{-}OSi(OH)_3^-$, strongly contribute in making this mechanistic sequence an attractive one.

If we subtract out the influence of the catalyst, $Si(OH)_5^-$, the energy for the condensation of silicic acid to the disiloxane, eq 7, is −2.86 kcal/mol. This compares with values near −15 kcal/mol for other estimates of this process.[32a,c]

$$2Si(OH)_4 \rightarrow (HO)_3SiOSi(OH)_3 + H_2O \quad (7)$$

Structural Details. The geometry about the Si atom in **1** can be referred to a trigonal bipyramid (TBP) with F1 and F2 in axial positions. The atoms of the equatorial plane, Si, F3, C11, and C21, are coplanar to within ±0.019 Å, while the atoms Si, F1, F2, and F3 are coplanar to within ±0.013 Å. The dihedral angle between these planes is 89.7°. Deviations from the idealized TBP geometry are not toward a rectangular pyramid and most likely reflect the larger steric requirements of the mesityl groups relative to the fluorine atoms. The angle between the mesityl groups (C11–Si–C21) is opened up to 127.0 (4)° compared to the ideal value of 120°, while the axial fluorine atoms are bent away from these groups toward the equatorial F3 atom (F1–Si–F2 = 175.6 (3)°). The mesityl ligands are rotated about 35° out of the equatorial plane (dihedral angles of 32.8° and 36.6° for the planes C11–C16 and C21–C26, respectively). This arrangement serves to stagger the ortho methyl groups of the mesityl ligands between adjacent axial–equatorial substituents on silicon and to mitigate contact between C19 and C27 (3.51 (1) Å compared to the van der Waals' sum of 4.0 Å[34] for two methyl groups). Short F-methyl contacts in the molecule are C17–F1 = 2.98 (1) Å, C17–F2 = 3.12 (1) Å, C29–F2 = 2.93 (1) Å, and C29–F3 = 3.10 (1) Å; all compared to the van der Waals' sum of 3.35 Å. As is expected the equatorial Si–F3 bond length of 1.641 (6) Å is somewhat shorter than the $Si\text{–}F_{axial}$ bond lengths: Si–F2 = 1.678 (6) Å, Si–F1 = 1.729 (6) Å. The larger value of the latter reflects a bonding interaction of F1 with the potassium ion of the cation. The distance K–F1 is 2.549 (4) Å which is comparable to the K–F distance of 2.67 Å in potassium fluoride.[35] The potassium ion of the cation is roughly equidistant from the six oxygen atoms, with K–O distances ranging from 2.804 (8) to 2.942 (9) Å. These values are somewhat larger than the sum of the van der Waals' radius for O and the ionic radius of K^+ (2.73 Å).[36]

The basic structural entity in **2** is the $[Mes_2Si(F)O]^-$ anion. Since there is only one NEt_4^+ cation for each pair of anions, a proton is necessary to maintain electrical neutrality. Inversion-related anions are oriented so that the O–O′ distance across the inversion center is 2.434 (7) Å.

This surprisingly short distance is less than the van der Waals' sum of 2.8 Å and is comparable to the O–O distance found for the very short O–H–O bonds in acid salts of carboxylic acids which are believed to be symmetric.[37] It seems reasonable to conclude that the proton which is required to maintain electrical neutrality is involved in a strong and possibly symmetric hydrogen-bonding interaction with O and O′. In the event that the hydrogen atom is truly centered between O and O′, it would lie on a crystallographic inversion center. Such symmetry is believed to favor the formation of symmetric hydrogen bonds.[37]

It is interesting to note that the maximum residual density on the final difference Fourier synthesis (0.32 e/Å^3) lies on an inversion center at a distance of 1.217 (4) Å from a pair of inversion-related oxygen atoms. A proton is not a hydrogen atom in that it has no formal electron density. It would be expected that electron density would accrue in the orbitals of a proton so located between two oxygen centers, but it is not clear that the scattering factors for a neutral H atom are appropriate. In addition, the location of the proton is suspect in that a pair of electron density maxima somewhat off of the inversion center could combine to cause a maximum to appear there. Therefore we elected to omit the proton from the refinement.

The geometry about the Si atom in the anion is essentially tetrahedral. The largest angular deviations from ideal geometry are O–Si–C11 = 117.1 (4)° and F1–Si–C11 = 100.9 (3)°. The larger value of the former may result from a mitigation of the crowding between methyl group C17 and the oxygen atom. The atoms Si, O, and C11–C16 are coplanar to within ±0.075 Å, an arrangement which minimizes the distance between C17 and O (3.05 (1) Å). The hydrogen atoms bonded to C17 appear to be staggered relative to the O atom (H171–O = 2.751 Å, H173–O = 2.697 Å).

In contrast to the coplanarity of the Si–O bond with the mesityl group C11, the mesityl group C1 is rotated 26.7° out of the plane defined by F1, Si, and C1. There is a short intramolecular contact between methyl group C7 and F1 (2.83 (1) Å) where hydrogen atom H71, bonded to C7, is 2.140 Å from F1 compared to the van der Waals' sum of 2.55 Å. This distance suggests a hydrogen bond between H71 and F1 with the formation of a six-membered ring.

The most surprising feature of the geometry is in the relative lengths of the Si–O and Si–F bonds which seem to be inverted. The Si–O bond length of 1.565 (6) Å is shorter than the value of 1.61 Å[38] for SiO_4^{4-}, while the Si–F1 bond length of 1.636 (5) Å is long compared to the values 1.54 Å for SiF_4[39] or 1.594 Å for SiH_3F. A hydrogen bond to F1 would be expected to increase the Si–F1 bond length. It is less clear why the Si–O bond appears to have so much implied double bond character.

The ether **3** has crystallographic C_2 symmetry, with the oxygen atom lying on the 2-fold axis. The Si–O–Si′ bond angle of 150.8 (2)° is large but comparable to the angle of 155° found in $O(SiH_3)_2$.[40] Unlike **2**, in this case both the O atom and the F atom lie roughly in planes defined by the two mesityl groups. The atoms Si, O, and C1–C6 are coplanar to within ±0.076 Å, while the atoms Si, F, and C11–C14 are coplanar to within ±0.067 Å. The dihedral angle between these planes is 86.2°. The aforementioned

(34) Pauling, L. *The Nature of the Chemical Bond*, 3rd. ed.; Cornell University Press: Ithaca, NY, 1960; p 260.
(35) Reference 34, p 520.
(36) Reference 34, p 514.
(37) Hamilton, W. C.; Ibers, J. A. *Hydrogen Bonding in Solids*; W. A. Benjamin, Inc.: New York, 1968; p 181.
(38) Reference 34, p 321.
(39) Reference 34, p 313.
(40) Wells, A. F. *Structural Inorganic Chemistry*, 3rd. ed.; Oxford University Press: London, 1962; p 58.

coplanarities minimize, in the absence of angular distortion, the distances between C7 and O (3.004 (4) Å) and C11 and F (2.860 (5) Å). In this case, the hydrogen atoms on C7 and C17 appear to be staggered with respect to O and F, respectively (H71–O = 2.685 Å, H73–O = 2.697 Å); H171–F = 2.486 Å, H173–F = 2.624 Å).

Acknowledgment. The support of this research by the National Science Foundation (Grant CHE85-04737) is gratefully acknowledged. We also thank the NSF and the San Diego Supercomputer Center for a generous allocation of computer time.

Supplementary Material Available: Tables of thermal parameters, hydrogen atom parameters, and additional bond lengths and angles (Tables SI–III for **1**, Tables IV–VI for **2**, and Tables VII–IX for **3**) (16 pages); tables of calculated and observed structure factors (38 pages). Ordering information is given on any current masthead page.

Synthesis of Alkylruthenium Nitrosyl Complexes. Migratory Insertion to Coordinated Nitric Oxide and the Mechanism of the Conversion of the Resultant Nitrosoalkyl Compounds to Oximate, Carboxamide, and Cyano Compounds

Jeffrey Chang, Mark D. Seidler, and Robert G. Bergman*

Contribution from the Department of Chemistry, University of California, Berkeley, California 94720. *Received August 11, 1988*

Abstract: The compounds (η^5-C_5Me_5)Ru(NO)R_2 (**2a**, R = CH_3; **2b**, R = CH_2CH_3) were synthesized by treating (η^5-C_5Me_5)Ru(NO)Cl_2 (**1**) with alkylating agents. Thermolysis of **2a** with PMe_3 gave (η^5-C_5Me_5)Ru$(PMe_3)_2$CN (**3**), H_2O, and CH_4; heating **2b** with PMe_3 produced (η^5-C_5Me_5)Ru((NO)$CHCH_3$)$(PMe_3)_2$ (**4**) and ethane. The reaction of **1** with PhMgCl followed by protonolysis with HCl gave (η^5-C_5Me_5)Ru(NO)(Ph)(Cl) (**5**); treatment of **5** with EtMgCl gave (η^5-C_5Me_5)-Ru(NO)(Ph)(Et) (**6**). Thermolysis of **6** with PMe_3 gave **4**; however, thermolysis of **6** with $PPhMe_2$ led to the NO insertion product (η^5-C_5Me_5)Ru(N(O)CH_2CH_3)(Ph)($PPhMe_2$) (**8**), characterized by X-ray diffraction (crystal data: space group $P2_1/c$; a = 8.6946 (6) Å, b = 10.749 (1) Å, c = 26.946 (3) Å, β = 95.7 (4)°; V = 2505.9 (8) Å^3; 3263 unique data, 2795 for which $F^2 > 3\sigma(F^2)$; R = 2.20%, wR = 2.98%, GOF = 1.88). Heating complex **8** with PMe_3 produced **4** while heating for extended periods with $PPhMe_2$ gave (η^5-C_5Me_5)Ru((NO)$CHCH_3$)$(PPhMe_2)_2$ (**9**). The conversion of **8** to **9** was found to proceed under milder conditions in the presence of a strong Brønsted base catalyst (e.g., $NaOSiMe_3$); using $CNBu^t$ in place of $PPhMe_2$ afforded (η^5-C_5Me_5)Ru((NO)$CHCH_3$)($PPhMe_2$)($CNBu^t$) (**11**). Treatment of **8** with the stronger base KN$(SiMe_3)_2$ in the presence of $PPhMe_2$ led to (η^5-C_5Me_5)Ru(Ph)$(PPhMe_2)_2$ (**12**) and $KONCHCH_3$. Reaction of **8** with KN$(SiMe_3)_2$ and 18-crown-6 gave [(η^5-C_5Me_5)Ru((NO)$CHCH_3$)(Ph)($PPhMe_2$)]$^-$[K^+·crown] (**13**). Complex **13** reacts with $PPhMe_2$ to give **12** and with Et_3SiOH and $PPhMe_2$ to generate **9**. Mechanistic studies, including kinetics, isotope effect, and tracer experiments, indicate that conversion of **8** to **4**, **9**, and **12** is initiated by the base abstraction of a methylene proton of the nitrosoethane ligand. Upon further thermolysis, **4** rearranges to (η^5-C_5Me_5)Ru(N(H)C(O)CH_3)$(PMe_3)_2$ (**14**). A possible mechanism for this transformation is discussed.

The discovery and elucidation of metal-mediated processes that form new bonds in organic compounds are important goals in organometallic chemistry. Partly in response to this, a significant amount of research has focused on the synthesis and reactivity of organotransition-metal nitrosyl compounds; among the desired properties of these complexes would be their reactions to form new carbon–nitrogen bonds.[1]

Considerable progress has been made in this area. Among the better understood C–N bond-forming reactions is migratory insertion of nitric oxide into metal–carbon bonds;[2] mechanistic studies[3] have established the close similarity of this reaction to the better known metal–carbonyl insertion reaction.[4] The unusual reaction between (η^5-C_5H_5)Co$(NO)_2$ and alkenes has also been thoroughly investigated.[5]

Studies of nitrosyl–transition metal compounds have proven useful in modeling the heterogenous metal-catalyzed oxidation of propene by NO to form acrylonitrile.[6] A group at Dupont has discovered[7] that η^3-allylnickel bromide dimer reacts with nitric oxide to form (η^2-CH_2=CHCH(NOH))Ni(NO)Br. In subsequent years, closely related chemistry of allyl and nitrosyl ligands was uncovered for other transition metals.[8]

Earlier, we communicated our initial results concerning the chemistry of some new alkylnitrosylruthenium compounds, the thermolysis of which produced unusual ruthenium cyanide, η^1-oximate, and η^1-carboxamide complexes.[9] Migratory insertion

(1) (a) Pandey, K. K. *Coord. Chem. Rev.* **1983**, *51*, 69–98. (b) Caulton, K. G. *Coord. Chem. Rev.* **1975**, *14*, 317–355.

(2) See, for example: (a) Wailes, P. C.; Weigold, H.; Bell, A. P. *J. Organomet. Chem.* **1972**, *34*, 155–164. (b) Fochi, G.; Floriani, C.; Chiesi-Villa, A.; Gaustini, C. *J. Chem. Soc., Dalton Trans.* **1986**, 445–447. (c) Jones, C. J.; McCleverty, J. A.; Rothin, A. S. *Ibid.* **1985**, 405–407. (d) Middleton, A. R.; Wilkinson, G. *Ibid.* **1981**, 1898–1905. (e) Middleton, A. R.; Wilkinson, G. *Ibid.* **1980**, 1888–1892. (f) Shortland, A. J.; Wilkinson, G. *Ibid.* **1973**, 872–876. (g) Klein, H.-F.; Karsch, H. H. *Chem. Ber.* **1976**, *109*, 1453–1464. (h) Goldhaber, A.; Vollhardt, K. P. C.; Walborsky, E. C.; Wolfgruber, M. *J. Am. Chem. Soc.* **1986**, *108*, 516–518.

(3) (a) Weiner, W. P.; Bergman, R. G. *J. Am. Chem. Soc.* **1983**, *105*, 3922–3929. (b) Weiner, W. P.; White, M. A.; Bergman, R. G. *Ibid.* **1981**, *103*, 3612–3614. (c) Seidler, M. D.; Bergman, R. G. *Organometallics* **1983**, *2*, 1897–1899. (d) Diel, B. N. *J. Organomet. Chem.* **1985**, *284*, 257–262.

(4) (a) Kuhlmann, E. J.; Alexander, J. J. *Coord. Chem. Rev.* **1980**, *33*, 195–225. (b) Calderazzo, F. *Angew. Chem., Int. Ed. Engl.* **1977**, *16*, 299–311.

(5) Becker, P. N.; Bergman, R. G. *J. Am. Chem. Soc.* **1983**, *105*, 2985–2995 and references therein.

(6) (a) England, D. C.; Mock, G. V. U.S. Patent 2736739, 1956. (b) England, D. C.; Foster, R. E. U.S. Patent 3023226, 1962. (c) Arai, H.; Iida, H.; Kunugi, T. *J. Catal.* **1970**, *17*, 396–398.

(7) (a) Clement, R. A. U.S. Patent 3652620, 1972. (b) Clement, R. A.; Klabunde, U.; Parshall, G. W. *J. Mol. Catal.* **1978**, *4*, 87–94.

(8) Schoonover, M. W.; Baker, E. C.; Eisenberg, R. *J. Am. Chem. Soc.* **1979**, *101*, 1880–1882 and references therein.

0002-7863/89/1511-3258$01.50/0